Ultraslow relaxation of hydrogen-bonded dynamic clusters in glass-forming aqueous glucose solutions: A light scattering study

D. L. Sidebottom
Department of Physics, Creighton University, Omaha, Nebraska 68178, USA
(Received 9 January 2007; revised manuscript received 24 March 2007; published 10 July 2007)

We report static and dynamic light-scattering measurements of aqueous glucose solutions near their glass transition. Photon correlation spectroscopy reveals two relaxation processes present in the supercooled liquid: a nonexponential and nonhydrodynamic, α-relaxation occurring at short times and an exponential and hydrodynamic relaxation occurring at longer times. The slow relaxation is seen only in the polarized scattering geometry and is in many ways identical to the "ultraslow" mode recently observed by others in specially annealed molecular glass-forming liquids and attributed to the formation of long-range density correlations or "dynamic clusters." Static light scattering confirms the existence of excess scattering in our glucose solutions that is consistent with clusters in a size range between 30 and 60 nm. The size of the clusters varies with the water content and the clustering appears to be associated with the percolation of a hydrogen-bonded glucose network.

DOI: 10.1103/PhysRevE.76.011505 PACS number(s): 64.70.Pf, 78.35.+c

I. INTRODUCTION

The ability to vitrify an aqueous solution is critically important to the field of biopreservation. While many inorganic salt solutions can often be vitrified [1], particular interest for cryobiological applications concerns those organic-based glass-forming aqueous solutions that are more likely to be biocompatible [2–6]. The prime candidate among these are the many aqueous sugar solutions that feature prominently in the cryopreservation of biological tissues in nature. Many animals in winter survive freezing weather by producing glucose, or other natural sugars (e.g., trehalose), within their bodies to act as an antifreeze [7,8]. The most commonly cited example is the wood frog who freezes solid in winter but returns to life during the spring thaw [9]. At the onset of cold temperatures, glucose produced by the liver circulates throughout the body. In addition to stabilizing proteins [10], the glass-forming properties the glucose reduces the likelihood that ice will form inside cells or capillaries. Should this crystallization occur, the rapid expansion would rupture the cell membrane or otherwise destroy the delicate internal components [9].

The glass transition from a liquid to an amorphous solid occurs in a wide variety of materials but is still one of the largely unsolved subjects of condensed matter physics [11,12]. The transition is characterized by a slowing of the viscoelastic relaxation of the liquid with cooling until a temperature T_g is reached at which the characteristic relaxation time exceeds common human timescales. Below T_g the material appears solid by most any conventional measure. The relaxation time is generally non-Arrhenius and often described by the empirical expression

$$\tau = \tau_0 \exp\left\{\frac{E}{k_B(T-T_0)}\right\}, \tag{1}$$

which diverges at a temperature T_0 that is typically some 50 K below T_g [13]. The degree of non-Arrhenius temperature dependence of the relaxation time varies from material to material. In fact, it was shown some years previously that the non-Arrehenius behavior is most noticeable in simple molecular liquids and polymers while a near Arrhenius (i.e., $T_0 \approx 0$) temperature dependence is seen in covalently bonded network-forming oxide glasses. This spectrum of degrees of non-Arrhenius behavior is referred to as the fragility [12,13]. A customary measure of the fragility is the fragility index m, defined in terms of the slope of the relaxation time (or the shear viscosity) near T_g in an appropriately scaled Arrhenius plot,

$$m = \left.\frac{d\log_{10}(\tau/\tau_0)}{d(T_g/T)}\right|_{T=T_g}. \tag{2}$$

Another important feature of the viscoelastic relaxation near T_g is its nonexponential time dependence. The nonexponential character of the structural relaxation is often described by a stretched exponential,

$$S(q,t) = A\exp\{-(t/\tau)^{\beta}\}. \tag{3}$$

The stretching exponent β is less than 1 and varies with fragility [14]. For liquids of high fragility index ($m > 100$), β is much less than unity. For strong liquids of low fragility index ($m \approx 20$), β is nearly 1 and the relaxation is essentially exponential.

A handful of studies of the glass-forming properties of glucose solutions have appeared over the years including differential scanning calorimeter measurements [15] of the glass transition temperature and dielectric relaxation measurements [16] of the viscoelastic relaxation, as well as a number of molecular dynamics simulations [17–19]. However, we are unaware of any previous dynamic light-scattering measurements using photon correlation spectroscopy (PCS). Here we report results of a PCS study of aqueous glucose solutions in their viscoelastic regime at temperatures just above T_g. Concentrations range from between 9 mol % glucose to 59 mol % glucose. Interestingly, we observe two relaxations. At the shortest times we observe a q-independent (nonhydrodynamic) relaxation which is nonexponential and whose relaxation rate tracks the main vis-

coelastic relaxation as reported by dielectric studies. At longer times, we observe a nearly q^{-2}-dependent (hydrodynamic) relaxation that is exponential and whose relaxation rate merges with the faster relaxation at temperatures near T_g. This slower relaxation is in many respects similar to a slow exponential relaxation seen by others [20–22] in certain molecular liquids near T_g and attributed to long-range density correlations (i.e., glassy clusters). Here, however, our results indicate a percolation of hydrogen-bonded glucose in the vicinity of 30 mol % glucose and the slow relaxation is attributed to the diffusion of independent glucose clusters.

II. EXPERIMENT

Glucose solutions were prepared using reagent-grade (Fisher) D-glucose and de-ionized water (Milli-Q). First a stock solution of approximately 50 wt % was obtained by mixing the components in a beaker with a magnetic stirrer under gentle heating until completely dissolved. Approximately 20 ml of the stock solution was then filtered through a 0.22-μ Teflon filter (Millipore) directly into a precleaned and preweighed 25-ml Wheaton vial. The opening of the vial was fitted with a piece of lens tissue but otherwise left exposed to allow water to evaporate. Samples were placed in a small oven maintained a temperatures between 70 °C and 80 °C to evaporate the water without caramelizing the sugar. The samples were periodically weighed and removed from the oven when a desired concentration was reached. The vial was capped and stored in a refrigerator to help minimize premature crystallization when not in use.

Dynamic light scattering was conducted at a variety of temperatures above T_g. Samples were held in a brass block that was in thermal contact with a coil of copper tubing through which flowed coolant from a recirculating chiller. This arrangement provided temperature control to within 0.1 °C for temperatures from −15 °C to 80 °C. The vertically polarized light (532 nm) from a diode-pumped solid state laser (Coherent Verdi) was focussed onto the sample and the light scattered at 90° was passed through an interference filter (532±20 nm) and a Glans-Thomson polarizer before being focussed onto a 50-μ pinhole located approximately 50 cm from the active area of a low-dark-count photomultiplier tube (PMT) (EMI 9863B). The photopulses from the PMT were digitized and fed to a commercial correlator (Correlator.com) which computed the intensity-intensity autocorrelation function (ACF)

$$C(q,t) = \frac{\langle I(0)I(t)\rangle}{\langle I\rangle^2} = 1 + A_C|S(q,t)|^2, \tag{4}$$

where $S(q,t)$ is the dynamic structure factor (the normalized density correlation function) [23] and $q=(4\pi n/\lambda)\sin(\theta/2)$ is the scattering wave vector for quasielastic scattering of light of wavelength λ at an angle of θ from a sample with index of refraction n. The compositional dependence of the index of refraction was obtained by a straightforward interpolation of available data from the literature [24,25]. The parameter A_C (=0.71±0.03) is an instrumental constant [26] that was determined by scattering from dilute suspension of polystyrene spheres.

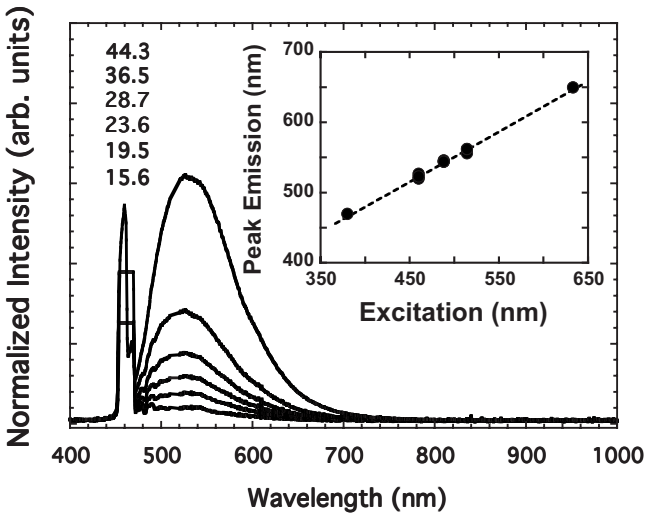

FIG. 1. Emission spectra for several aqueous glucose solutions (mol % glucose listed in order of peak intensity) excited by 460-nm laser light. The narrow peak at 460 nm is the laser line. The broad peak near 530 nm increases with increasing glucose content. Inset shows how the location of the peak emission intensity shifts in proportion to the excitation wavelength.

In addition to these temperature-dependent measurements, an angle-dependent study was also performed on samples maintained at room temperature. These included both measurements of the ACF and the static light scattered at angles from 90° to 14°.

III. RESULTS

During our initial work with concentrated samples, we visually noticed a high level of orange photoluminescence emanating from the sample when exposed to the laser light. This prompted a separate study in which emission spectra were recorded at a number of excitation wavelengths and varying glucose concentrations. An example of the emission spectra for samples of varying concentration with excitation at 460 nm is shown in Fig. 1. The intensity of the spectra has been normalized to the scattering from a control sample of polystyrene in water and shows a systematic increase in the emission peak with increasing glucose content. Furthermore, the peak emission wavelength shifts in proportion to the excitation (see inset to Fig. 1), suggesting that the emission might originate from Raman scattering of the water. Further details of our photoluminescence study are presented elsewhere [27]. In any event, to block this unwanted, inelastic scattering, we incorporated a reasonably wide band interference filter into the collection train.

Figure 2 shows examples of the ACF recorded for vertically polarized light scattered at 90° for a range of temperatures on a sample containing 37.0 mol % glucose. Clearly evident is the presence of two distinct relaxations whose time scales are well separated at high temperatures but appear to converge at lower temperatures. To characterize these two relaxations, we fit the ACFs to a weighted sum of two stretched exponentials:

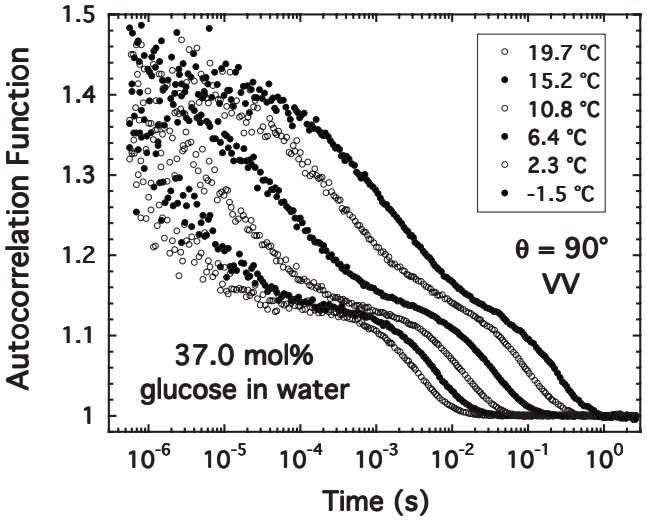

FIG. 2. Intensity autocorrelation functions obtained for VV scattering from an aqueous solution containing 37 mol % glucose at the temperatures listed showing the two relaxations discussed in the text.

$$C(q,t) = 1 + A_C|A_F \exp[-(t/\tau_F)^{\beta_F}] + A_S \exp[-(t/\tau_S)^{\beta_S}]|^2, \tag{5}$$

where the subscripts S and F refer to fast and slow relaxation, respectively. An example of the quality of the fitting is shown in Fig. 3 for a temperature of −1.5 °C. Also shown in Fig. 3 is the spectrum obtained for depolarized light scattered at 90°. We observed that the total scattering in the vertical-horizontal (VH) polarization was only about 20% of that found in the vertical-vertical (VV) polarization. Clearly absent in the VH spectra is the slow relaxation. Instead the relaxation present in the VH spectra appears to resemble the fast relaxation found in the VV spectra. Indeed, as we show

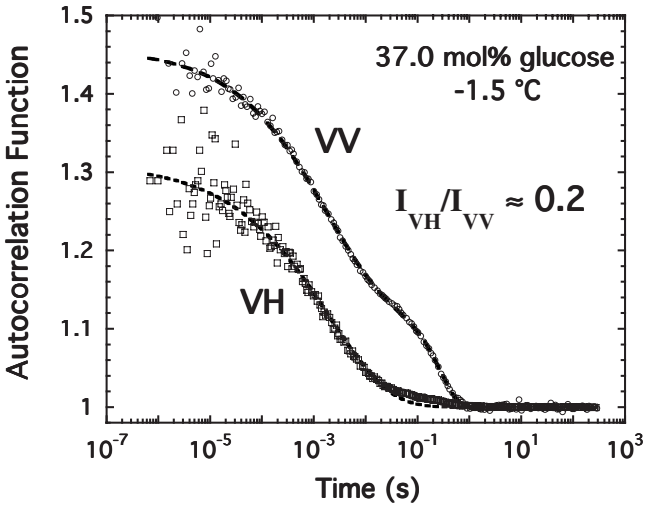

FIG. 3. Intensity autocorrelation function obtained for 37 mol % glucose solution at −1.5 °C in both the vertically polarized and depolarized scattering geometries. The VH spectra only exhibits the fast relaxation. The dashed lines are curve fits to Eq. (5).

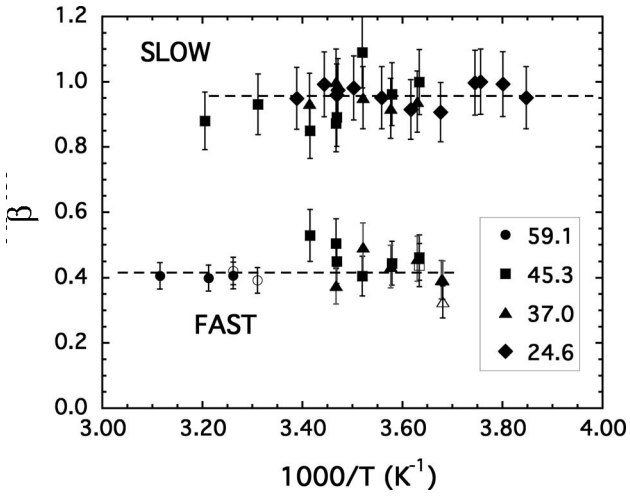

FIG. 4. Stretching exponent observed for the fast and slow relaxation as obtained from curve fits to Eq. (5). Key refers to the mol % glucose. Open symbols are fits to VH spectra.

momentarily, the curve fitting parameters support this assignment.

The results of the curve fitting are summarized in the next three figures. In Fig. 4, the stretching exponents β_S and β_F obtained from fitting Eq. (5) are presented. Here we see that the fast relaxation exhibits a nonexponential decay with $\beta_F \approx 0.45 \pm 0.05$. This is corroborated by the VH spectra in which only the fast relaxation is present and only three fit parameters are required. Furthermore, the observed stretching exponent is consistent with that obtained from the full width at half maximum (FWHM) of the dielectric loss spectra measured by Chan *et al.* [16]. The FWHM of the dielectric loss was reported to range between 2.3 and 2.7 decades, and this corresponds to $\beta \approx 1.14/(\text{FWHM})$ of 0.46 ± 0.04. In contrast to this nonexponential fast relaxation, the slow relaxation appears essentially exponential, $\beta_S \approx 0.95 \pm 0.1$. The error bars shown in Fig. 4 are chiefly a reflection of the large number of parameters involved in curve fitting the VV spectra.

Figure 5 presents the temperature variation of all the relevant relaxation times (τ_S and τ_F) plotted in an Arrhenius manner. Also included are those obtained from fitting of VH spectra. For compositions above 30 mol % glucose, we could observe both a fast and slow relaxation within the time window of our experiment and within our temperature limits. We see from Fig. 5 that the samples in this composition range exhibit roughly constant activation energies for both the fast and slow relaxations, respectively. The activation energy of the fast relaxation is 2.74 ± 0.05 eV and that of the slow relaxation is only 1.40 ± 0.02 eV. Consequently, the time scales of the two relaxations must converge at some temperature, and from Fig. 5 it is apparent that they converge near T_g, where the viscoelastic relaxation time approaches about 100 s. The glass transition temperatures and fragility indices of these concentrated samples are determined to be $T_g = 250.3$ K and $m = 56.5$ for 37 mol % glucose, $T_g = 254.7$ K and $m = 50.8$ for 45.3 mol % glucose, and $T_g = 283.4$ K and $m = 50.6$ for 59.1 mol % glucose.

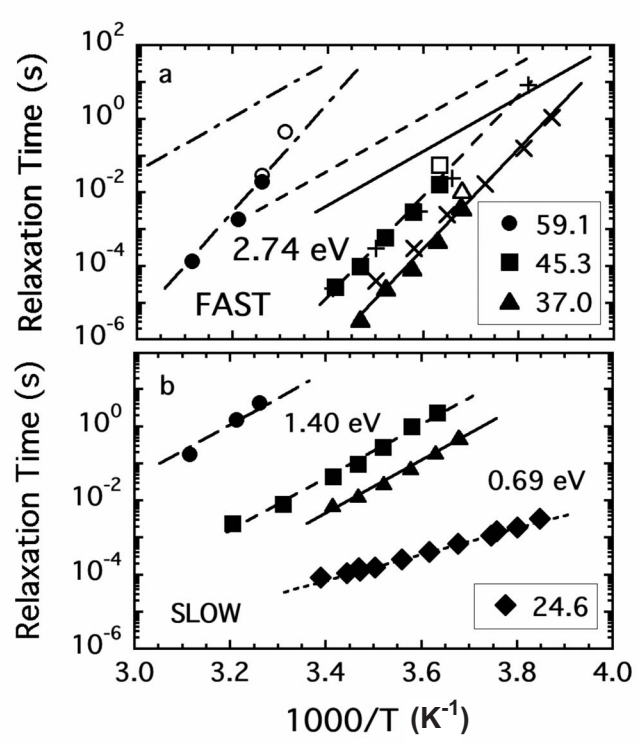

FIG. 5. Relaxation times for both the (a) fast and (b) slow relaxation as obtained from curve fits to Eq. (5). Key refers to the mol % glucose. Open symbols are fits to VH spectra. Lines are guides to the eye to indicate how the two relaxations appear to merge at temperatures near T_g. Also included are results from dielectric studies [16] for 36.2 mol % (crosses) and 47.4 mol % (pluses).

Included in Fig. 5 for comparison are results from dielectric relaxation measurements [16]. Plotted are the inverse of the frequency at which the dielectric loss maximum occurs for samples of 10 and 15 wt % water (47.4 and 36.2 mol % glucose, respectively). These agree favorably with our present fast relaxation for samples of 45.3 and 37.0 mol % glucose. Given this finding and our observation of nonexponential relaxation, we conclude that the fast relaxation present in our ACF is the so-called α-relaxation—that is, the main viscoelastic relaxation which most nearly tracks the shear viscosity of the liquid.

At compositions below 30 mol %, only the slow, exponential relaxation was observed. This could be merely a consequence of the temperature limitation in our present experiment which did not allow for cooling the samples below about −15 °C, but as we argue later, it might also be associated with the absence, at these dilute concentrations, of a continuous hydrogen-bonded glucose network whose structural relaxation gives rise to the fast viscoelastic relaxation. Additional evidence for a transition near 30 mol % is seen in the abrupt twofold decrease in the activation energy of the slow relaxation for our 24.6 mol % sample in comparison to that seen for samples containing higher concentrations of glucose.

Last, we consider the compositional variations of the two amplitudes A_S and A_F obtained in the curve fitting of Eq. (5).

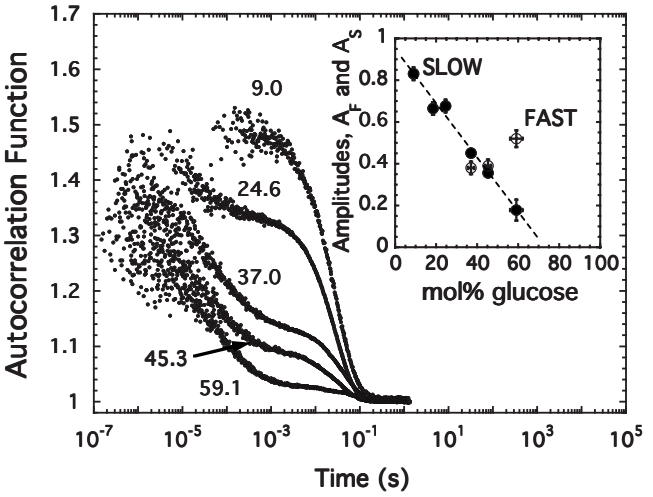

FIG. 6. A comparison of the amplitude variations of the autocorrelation functions for five concentrations listed in mol % glucose. Some spectra have been shifted horizontally for maximum clarity. Inset shows the amplitudes observed for the fast (open symbols) and slow (solid symbols) relaxation as obtained from curve fits to Eq. (5) plotted as a function of the glucose concentration.

Neither amplitude exhibited any appreciable temperature dependence, and in Fig. 6 we have plotted the autocorrelation functions obtained for five compositions to illustrate the how the amplitude of the slow relaxation systematically changes with changing glucose content. In the inset of Fig. 6 we plot the variation of both amplitudes A_S and A_F as a function of the glucose concentration. The fast relaxation, which was observed only at concentrations above 30 mol %, displays only a modest variation with composition, increasing slightly with increasing concentration. In contrast, the slow exponential relaxation decreases linearly with increasing concentration and appears to vanish in the vicinity of 70 mol % glucose.

At this point, let us consider the possible origins of the two relaxations. First, the fast relaxation exhibits all the properties of the main viscoelastic relaxation, being both nonexponential and coincident with the α-relaxation probed by dielectric spectroscopy [16]. In all respects, this fast relaxation is not unexpected. Rather, it is the slow relaxation that appears anomalous. Such slow relaxations could originate from the diffusion of small particulates in the sample that were not adequately removed by filtration [26], but alternatively they could indicate the presence of long-ranged density correlations (i.e., clusters) occurring in the liquid.

In their studies of glass-forming orthoterphenyl (OTP), Patkowski and co-workers [20–22] observed an exponential decay occurring at time scales that were some seven orders of magnitude slower than the viscoelastic relaxation time. This "ultraslow" relaxation was not present in all samples of OTP, but could be produced in samples that were specially annealed. Like our present slow relaxation, this exponential decay was only observed in the VV scattering geometry.

Patkowski *et al.* [20] concluded that the ultraslow relaxation was the result of the diffusion of glassy clusters (regions of higher density) of a size ranging from 100 to 300 nm that occur in the specially treated samples.

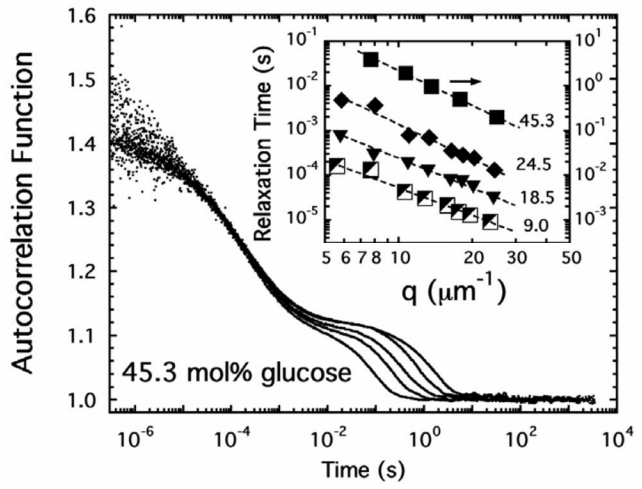

FIG. 7. Intensity autocorrelation functions obtained for VV scattering from an aqueous solution containing 45.3 mol % glucose at room temperature. Spectra are (from left to right) for scattering angles of 90°, 60°, 45°, 35°, and 25°. Inset shows the variation of the slow relaxation time with scattering wave vector for four samples with mol % glucose indicated.

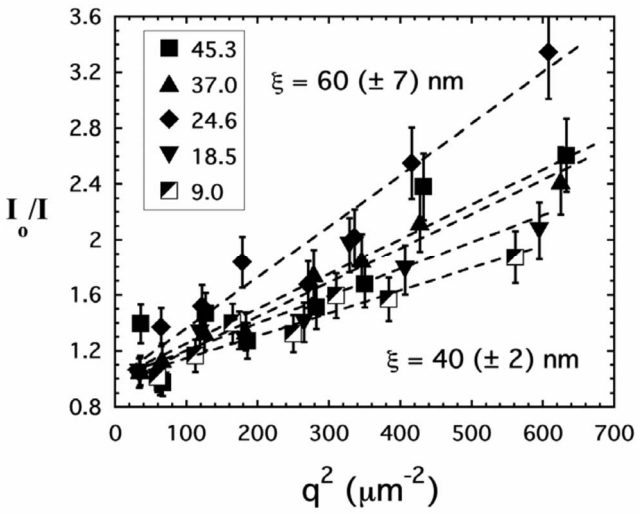

FIG. 8. Ornstein-Zernicke plot of the angular variation of the scattered light from samples of varying mol % glucose. Dashed lines are fits to Eq. (7). The extremes of correlation length are indicated in the figure.

The diffusion of these clusters is believed to occur through diffusion of their boundaries—that is, a mechanism in which the boundary is locally growing and melting without any mass transport involving the inner parts of the cluster [22]. Support for this assignment came from both dynamic and static light scattering conducted at varying scattering angles which showed a nearly q^{-2} dependence for the relaxation time of the ultraslow mode and indicated long-range density correlations with a size of order 100 nm [20].

But could we be observing the diffusion of small particulates (i.e., dirt)? There are several reasons for why we do not believe this to be the case. First, the visible appearance of the scattered beam in our samples is homogenous and exhibits none of the coarse-grained appearance that is the hallmark of a dirty sample. Second, if dirt particles were the source of the slow mode, we would expect their relaxation time to parallel that of the viscous relaxation time (i.e., the fast mode). Instead the two time scales appear to be merging in the vicinity of T_g. We conclude then that our samples are well filtered and we have pursued additional angular studies of the scattering to explore the possibility that the slow relaxation is produced by long-range density correlations similar to those reported in molecular liquids.

Figure 7 shows the ACFs for our 45.3 mol % glucose sample measured at room temperature for five scattering angles from 90° to 25°. Two things are immediately evident. First, the fast relaxation is q independent. This is yet further confirmation that our fast mode is the α-relaxation as it is well known to be a q-independent, nonhydrodynamic mode in this low-q limit. Second, we find that the slow mode is q dependent. Its shape remains exponential and its relaxation time increases with decreasing scattering wave vector. As shown by the double-logarithmic inset to Fig. 7, the relaxation time varies as q^{-n} with n ranging from 2.1 ± 0.1 for the dilute solutions to 2.5 ± 0.1 for the more concentrated samples. These values of n are similar to those reported by Patkowski *et al.* [20] for OTP and are consistent with the diffusional motion of an agglomerated, fractal region of higher density.

We have also performed static light scattering on our samples and, like Patkowski *et al.* [20], we observed excess scattering in the forward direction. According to Patkowski *et al.*, the excess scattering results from correlated regions (the glassy clusters) whose radial distribution function may be approximated by [22]

$$g(r) \propto (1/r)\exp(-r/\xi), \tag{6}$$

with the resulting structure factor given by the Ornstein-Zernike formula [20]

$$S(q) = \frac{I(q)}{I(0)} = \frac{1}{1+q^2\xi^2}, \tag{7}$$

where ξ is the correlation length, a measure of the size of the clusters.

In Fig. 8 the inverse scattered intensity is plotted against q^2 in the fashion of Ornstein and Zernicke. The intensity in the limit of $q=0$ was estimated by extrapolation of $I(q)^{-1}$ to $q=0$. From the slopes of the best linear fits to data in Fig. 8, we find correlation lengths that range from 40 ± 2 nm to 60 ± 7 nm. These values are somewhat smaller but not unlike those ($\approx$100 nm) reported by Patkowski *et al.* for a series of cluster-containing liquids. The variation of the correlation length with glucose concentration is shown in Fig. 9. Evident in the figure is an initial increase in the correlation length with increasing glucose concentration reaching a maximum cluster size in the vicinity of 30 mol % before then decreasing.

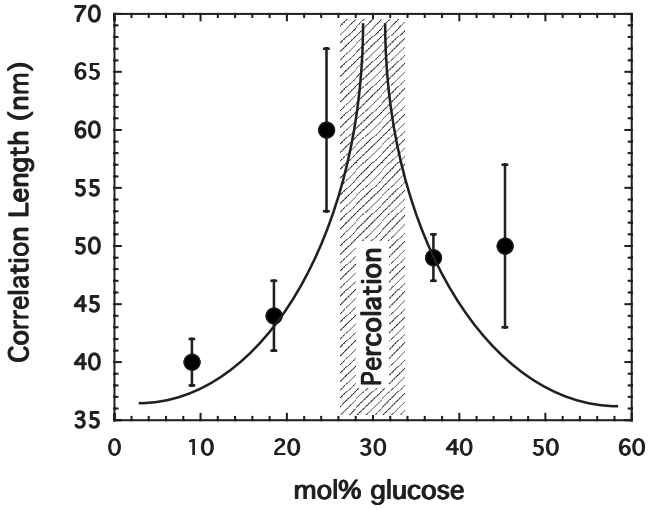

FIG. 9. Variation of the correlation length of glucose clusters with respect to mol % glucose as obtained from analysis of the static light-scattering measurements shown in Fig. 8. Lines are only shown to suggest the correspondence to a percolation transition near 30 mol % glucose.

IV. DISCUSSION

Let us begin our discussion by reiterating that we observe two relaxations. The first, occurring at short times, is the α-relaxation. That is, it is the q-independent, nonexponential, viscoelastic relaxation that epitomizes the glass transition itself. The second relaxation, occurring at longer times, appears to be a hydrodynamic mode resulting from the diffusion of clusters (agglomerated regions of matter) within the melt. In every respect this latter relaxation shares identical properties with the ultraslow mode reported by Patkowski and co-workers [20–22] for a variety of properly prepared glass-forming molecular liquids.

However, there are some novel features in the present study. In the molecular liquids of Patkowski *et al.*, the ultraslow mode occurred on time scales that were some six to nine orders of magnitude slower than the α-relaxation [20]. Consequently, only one of the two relaxations could be observed by the correlator (a time window ranging from about 1 μs to tens of seconds) in any given autocorrelation spectrum. This made it considerably more challenging to assess the relative amplitudes of the two relaxation modes. In fact, in later work Patkowski *et al.* employed ensemble-averaging techniques [21] to accurately assess the amplitude of the α-relaxation. Here, we find both relaxations present within our time window and can monitor changes in both the relaxation time and the relative amplitudes of each relaxation without the necessity of employing ensemble-averaging techniques. Unlike the ultraslow mode seen by Patkowski *et al.* in the molecular liquids whose relaxation time was observed to parallel that of the α-relaxation [22], we instead observe the two relaxation times converging near T_g in the aqueous glucose system.

Another significant difference between the present clusters and those observed in the molecular liquids arises from the compositional variations that exist in our two-component system. Four specific features merit special consideration. The first is the compositional variation of the correlation length shown in Fig. 9 which displays a maximum at approximately 30 mol % glucose. The second is the abrupt change in the activation energy of the slow mode occurring near 30 mol % glucose. The third is the absence of the viscoelastic fast mode at concentrations below about 30 mol %. And the fourth notable feature is the amplitude of the slow relaxation shown in the inset to Fig. 6 which vanishes around 70 mol % glucose.

We believe that these features are symbolic of the important role played by hydrogen bonding in our aqueous glucose systems. Monosaccharides like glucose contain both hydrophilic hydroxl groups and hydrophobic hydrogen sites [28]. The precise conformation of the sites depends upon the sugar, but for glucose there are five such hydroxyl sites. Estimations of the hydration number for dilute glucose solutions range from 8 to 10 mol/mol [29] and molecular dynamics (MD) simulations suggest this number decreases with increasing glucose concentration [18]. It has often been remarked that the hydrogen bonding between sugar and water is stronger than that between water itself [17,28]. Not only are water-glucose bonds favorable, but with increasing glucose content, MD simulations indicate that a growing percentage of glucose-glucose hydrogen bonds begin to form. Indeed, Roberts and Debenedetti [18] suggest a percolation of a glucose network occurring in the vicinity of 60–80 wt % carbohydrate (about 16–30 mol % glucose) which leads to the trapping of water into small isolated "pockets." Thus we believe that much of our experimental findings can be simply interpreted in terms of the growth, agglomeration, and eventual percolation of hydrogen-bonded glucose clusters.

In the dilute regime, a large density of small clusters are formed. These scatter light much in the fashion of independently diffusing macromolecules in a solvent. The relaxation is exponential with a relaxation time that is essentially q^{-2} dependent owing to the Brownian diffusion of these particles in solution. The likely fractal morphology of these randomly formed clusters would result in a slightly higher $q^{-2.3\pm0.2}$ dependence such as we observe. The amplitude of the observed relaxation is proportional to the number density of the scatters [30]; that is, the number density of clusters with a mean cluster size, ξ. As the glucose content is increased, the mean cluster size increases, partly due to the increased number of glucose molecules available, but more significantly due to the agglomeration of *several* midsized clusters into a *single* even larger-sized cluster. This is a fundamental feature of the percolation process. Although the concentration of glucose has increased, the number density of these larger, agglomerated clusters has actually decreased [30]. It is for this reason the amplitude of the slow relaxation decreases (see inset to Fig. 6).

In the concentration range below 30 mol %, these independent clusters diffuse about with a relaxation time whose rather low activation energy is a reflection of the unpercolated state of the fluid. Eventually, the clusters grow sufficiently large so as to percolate a continuous network of hydrogen-bonded glucose within the system. It is at these concentrations where the viscoelastic relaxation of the gel

network gives rise to the nonexponential and q-independent fast-relaxation mode.

What then happens to the slow relaxation at concentrations above the 30 mol % percolation threshold? While there remain some independent glucose clusters, trapped in pockets of water within the gel network, the mean size of these isolated clusters now decreases as the largest-sized ones are quickly assimilated into the gel network [30]. Not only does the mean size decrease (see Fig. 9), but the number density of the isolated clusters decreases, resulting in the continued decrease in the amplitude of the slow relaxation. Furthermore, the diffusion of these few remaining isolated clusters must now take place within the confines of increasingly smaller pockets of water where MD simulations suggest that considerable slowing of the water dynamics occurs [29]. This we believe would account for the increased activation energy we observe for the slow mode at concentrations above 30 mol %.

In conclusion, our static and dynamic light-scattering results for aqueous glucose solutions indicate the presence of dynamic clusters in the vicinity of the glass transition. Such clusters have been previously reported for simple molecular glass-forming liquids, but this is the first report of such clusters occurring in glucose solutions. Unlike the molecular glass-forming liquids, the clusters in the aqueous glucose solutions occur as a direct consequence of intermolecular hydrogen bonding of glucose and the development of a percolated network of hydrogen-bonded glucose at a threshold composition. This leads to unique compositional variations in the cluster size and number density which can be monitored in our experiment. The formation of hydrogen-bonded clusters in these concentrated solutions suggests that glucose (and likely other natural sugars) possess the necessary structure and functionality to discourage crystallization and protect delicate biological tissues during freezing.

In future work, we plan to extend the temperature limits of our cryostat so as to study a wider range of compositions and plan to perform similar studies of other sugars (e.g., trehalose and/or maltose).

ACKNOWLEDGMENTS

Funding by the Petroleum Research Fund (Grant No. 43743-GB10) and Research Corporation (Award No. CC6641) is gratefully acknowledged as is the laboratory contributions of Nadia Akhtar.

[1] C. A. Angell, Chem. Rev. (Washington, D.C.) **102**, 2627 (2002).
[2] C. A. Angell, J. Non-Cryst. Solids **131–133**, 13 (1991).
[3] S. Magazu, P. Migliardo, A. M. Musolino, and M. T. Sciortino, J. Phys. Chem. B **101**, 2348 (1997).
[4] S. Magazu, G. Maisano, H. D. Middendorf, P. Migliardo, A. M. Musolino, and V. Villari, J. Phys. Chem. B **102**, 2060 (1998).
[5] C. Branca, S. Magazu, G. Maisano, P. Migliardo, V. Villari, and A. P. Sokolov, J. Phys.: Condens. Matter **11**, 3823 (1999).
[6] C. Branca, S. Magazu, G. Maisano, and F. Migliardo, Phys. Rev. B **64**, 224204 (2001).
[7] J. H. Crowe, J. F. Carpenter, and L. M. Crowe, Annu. Rev. Physiol. **60**, 73 (1998).
[8] J. H. Crowe and L. M. Crowe, Science **223**, 701 (1984).
[9] K. B. Storey and J. M. Storey, Annu. Rev. Ecol. Syst. **27**, 365 (1996).
[10] S. N. Timasheff, Annu. Rev. Biophys. Biomol. Struct. **22**, 67 (1993).
[11] P. G. Debenedetti and F. H. Stillinger, Nature (London) **410**, 259 (2001).
[12] M. D. Ediger, C. A. Angell, and S. R. Nagel, J. Phys. Chem. **100**, 13200 (1996).
[13] C. A. Angell, in *Relaxations in Complex Systems* (Proceedings of the Workshop on Relaxation Processes, Blacksburg, VA, July 1983), edited by K. Ngai and G. B. Wright (National Information Service, U. S. Department of Commerce, Washington, DC, 1985), p. 3.
[14] R. Bohmer, K. L. Ngai, C. A. Angell, and D. J. Plazek, J. Chem. Phys. **99**, 4201 (1993).
[15] J. L. Green and C. A. Angell, J. Phys. Chem. **93**, 2880 (1989).
[16] R. K. Chan, K. Pathmanathan, and G. P. Johari, J. Phys. Chem. **90**, 6358 (1986).
[17] E. R. Caffarena and J. R. Grigera, Carbohydr. Res. **300**, 51 (1997); **315**, 63 (1999).
[18] C. J. Roberts and P. G. Debenedetti, J. Phys. Chem. B **103**, 7308 (1999).
[19] N. C. Ekdawi-Sever, P. B. Conrad, and J. J. de Pablo, J. Phys. Chem. A **105**, 734 (2001).
[20] A. Patkowski, Th. Thurn-Albrecht, E. Banachowicz, W. Steffen, P. Bosecke, T. Narayanan, and E. W. Fischer, Phys. Rev. E **61**, 6909 (2000).
[21] A. Patkowski, H. Glaser, T. Kanaya, and E. W. Fischer, Phys. Rev. E **64**, 031503 (2001).
[22] A. Patkowski, E. W. Fischer, W. Steffen, H. Glaser, M. Baumann, T. Ruths, and G. Meier, Phys. Rev. E **63**, 061503 (2001).
[23] B. J. Berne and R. Pecora, *Dynamic Light Scattering* (Wiley, New York, 1976).
[24] *Handbook of Chemistry and Physics*, 64th ed. (CRC Press, Boca Raton, FL, 1985).
[25] G. S. Parks, H. M. Huffman, and F. R. Cattoir, J. Phys. Chem. **32**, 1366 (1928).
[26] N. C. Ford, Jr., in *Dynamic Light Scattering*, edited by R. Pecora (Plenum Press, New York, 1985) p. 7.
[27] N. Ahktar and D. L. Sidebottom (unpublished).
[28] A. Sugget, in *Water: A Comprehensive Treatise*, edited by F. Franks (Plenum Press, New York, 1975), Vol. 4.
[29] S. L. Lee, P. G. Debenedetti, and J. R. Errington, J. Chem. Phys. **122**, 204511 (2005).
[30] D. Stauffer, *Introduction to Percolation Theory* (Taylor & Francis, Philadelphia, 1985).